REVISITING THE LIQUID FLUIDIZED BED LAYER INVERSION PHENOMENA WITH COMPUTATIONAL FLUID DYNAMICS

Alexandre M S Costa, amscosta@uem.br
Jean R. Bocca
Paulo R. Paraíso
Luiz M M Jorge
Universidade Estadual de Maringá Av. Colombo 5790, bloco 104 , Maringá, PR, 87020-900

Abstract. *Solids mixing and segregation happens in liquid fluidized beds containing binary mixtures differing by density and size. The solid layer inversion occurs in a binary mixture when solids with greater size and smaller density reverse their relative vertical position, i.e. goes to the bottom, in the bed as the liquid velocity is increased In this work, we revisit the methodology of Syamlal and O´Brien (1988) using CFD and based on the Moritomi et al.(1982). experiments. The goal of our work is to compare the capabilities of new CFD models for polidisperse systems available in the literature in predicting and accurately describing aspects of the inversion phenomenon.*

Keywords*: fluidized beds, computational fluid dynamics, MFIX*

1. INTRODUCTION

Consider a binary solids system of spheres with a diameter and density referred as d_1, d_2 and ρ_{s1} and ρ_{s2}, correspondingly additionally consider that their size ratio and density ratio, are such as $d_1/d_2 > 1$ and $\rho_{s1}/\rho_{s2} < 1$. In this situation, at low velocities is possible to have segregation by density with solid 1 at the bottom of the bed, and at higher velocities segregation by size with solid 1 at the top of the bed. The previous phenomenon is termed "layer inversion", i.e., the lighter material (solids 1) now resides at the bottom of the bed. Based on experimental observations, Moritomi et al. (1982) verified the phenomenon besides happening with liquid velocity variation, could happen with solids composition variation for a constant liquid velocity.

Many papers have been published on the inversion phenomenon of binary-solid liquid fluidized beds. The work by Escudié et. al. (2006) provides a comparison of theoretical models for predicting the inversion phenomenon. According to them, the best agreements with experiments were within the ± 14 % range for the best models. In this work, we revisit the methodology of Syamlal and O´Brien (1988) using CFD and based on the Moritomi et al.(1982). experiments. The goal of our work is to compare the capabilities of new CFD models for polidisperse systems available in the literature in predicting and accurately describing aspects of the inversion phenomenon.

2. TWO FLUID MODEL

The mathematical model is based on the assumption that the phases can be mathematically described as interpenetrating continua; the point variables are averaged over a region that is large compared with the particle spacing but much smaller than the flow domain (see Anderson, 1967). A short summary of the equations solved by the numerical code in this study are presented next. Refer to Benyahia et al. (2006) , Syamlal et al. (1993) and Syamlal and Pannala (2011) for more detailment.

The continuity equations for the fluid and solid phase are given by :

$$\frac{\partial}{\partial t}\left(\varepsilon_f \rho_f\right) + \nabla\bullet\left(\varepsilon_f \rho_f \vec{v}_f\right) = 0 \tag{1}$$

$$\frac{\partial}{\partial t}\left(\varepsilon_m \rho_m\right) + \nabla\bullet\left(\varepsilon_m \rho_m \vec{v}_m\right) = 0 \tag{2}$$

In the previous equations ε_f, ε_m, ρ_f, ρ_m, $\vec{v}_f$ and $\vec{v}_m$ are the volumetric fraction, density and velocity field for the fluid and solids phases.

The momentum equations for the fluid and solid phases are given by:

$$\frac{\partial}{\partial t}\left(\varepsilon_f \rho_f \vec{v}_f\right) + \nabla\bullet\left(\varepsilon_f \rho_f \vec{v}_f \vec{v}_f\right) = \nabla\bullet\bar{\bar{S}}_f + \varepsilon_f \rho_f \vec{g} - \sum_{m=1}^{M} \vec{I}_{fm} \tag{3}$$

$$\frac{\partial}{\partial t}\left(\varepsilon_m \rho_m \vec{v}_m\right) + \nabla\bullet\left(\varepsilon_m \rho_m \vec{v}_m \vec{v}_m\right) = \nabla\bullet\bar{\bar{S}}_m + \varepsilon_m \rho_m \vec{g} + \vec{I}_{fm} - \sum_{\substack{k=1 \\ k\neq m}}^{M} \vec{I}_{km} \tag{4}$$

$\bar{\bar{S}}_f$ $\bar{\bar{S}}_m$ are the stress tensors for the fluid and solid phase. It is assumed newtonian behavior for the fluid and solid phases, i.e.,

$$\bar{\bar{S}} = \left(-P + \lambda\, \nabla\bullet\vec{v}\right)\bar{\bar{I}} + 2\mu\, S_{ij} \equiv -p\,\bar{\bar{I}} + \bar{\bar{\tau}} \qquad S_{ij} = \frac{1}{2}\left[\nabla\vec{v} + \left(\nabla\vec{v}\right)^T\right] - \frac{1}{3}\nabla\bullet\vec{v} \tag{5}$$

In the above equation *P, λ, μ* are the pressure, bulk and dynamic viscosity, respectively.

In addition, the solid phase behavior is apportioned between a plastic regime (also named as slow shearing frictional regime) and a viscous regime (also named as rapidly shearing regime). The constitutive relations for the plastic regime are related to the soil mechanic's theory. Here they are represented as:

$$p_m^p = f_1\left(\varepsilon^*, \varepsilon_f\right) \qquad \mu_m^p = f_2\left(\varepsilon^*, \varepsilon_f, \Phi\right) \tag{6}$$

In the above equation ε^* is the packed bed void fraction and Φ is the angle of internal friction.

A detailing of functions f_1 to f_9 can be obtained in Benyahia (2008).

On the other hand, the viscous regime behavior for the solid phase is ruled by two gas kinetic theory related parameters (e_m , Θ_m).

$$p_m^v = f_3\left(\varepsilon_m, \rho_m, d_{pm}, \Theta_m, e_m\right) \qquad \mu_m^v = f_4\left(\varepsilon_m, \rho_m, d_{pm}, \Theta_m^{1/2}, e_m\right) \tag{7}$$

The solid stress model outlined by Eqs. (6) and (7) will be quoted here as the standard model. Additionally, according to Pannala et al.(2009), a general formulation for the solids phase stress tensor that admits a transition between the two regimes using a weighting parameter "ϕ" is given by :

$$\bar{\bar{S}}_m = \begin{cases} \phi\left(\varepsilon_f\right)\bar{\bar{S}}_m^v + \left[1-\phi\left(\varepsilon_f\right)\right]\bar{\bar{S}}_m^p & \text{if } \varepsilon_f < \varepsilon^* + \delta \\ \bar{\bar{S}}_m^v & \text{if } \varepsilon_f \geq \varepsilon^* + \delta \end{cases} \tag{8}$$

In Eq. (3) the last term on the right hand side is the total momentum interaction between the fluid and solid phase. Also, $\vec{I}_{fm}$ in the summation is the momentum interaction term between the solid phase m and fluid phase, given by

$$\vec{I}_{fm} = -\varepsilon_g \nabla P_f - \beta_{fm}\left(\vec{v}_m - \vec{v}_f\right) \tag{9}$$

There are a number of correlations for the drag coefficient β. All can be recast in the form :

$$\beta_{fm} = \beta_{fm}\left(\varepsilon_f, d_{pm}, \rho_f, \mu_f, \left|\vec{v}_f - \vec{v}_m\right|\right) \tag{10}$$

In the Eq. (4), the last term in the right hand side stands for the total momentum interaction between and phase solid m and every other solid phase. Each term in the summation is given by :

$$\vec{I}_{km} = \varepsilon_m \nabla P_f + \beta_{km}\left(\vec{v}_k - \vec{v}_m\right) \tag{11}$$

Where :

$$\beta_{km} = \beta_{km}\left(\rho_k, \rho_m, \left|\vec{v}_k - \vec{v}_m\right|, e_{km}, g_{0,km}\right) \tag{12}$$

For closing the model, a transport equation for the granular energy Θ provides a way of determine the pressure and viscosity for the solid phase during the viscous regime. Equation (13) is a transport equation for the granular energy Θ. The terms κ_s γ and ϕ_{gs} are the granular energy conductivity, dissipation and exchange, respectively. Equation (14) presents their functional form.

$$\frac{3}{2}\left[\frac{\partial}{\partial t}\varepsilon_m \rho_m \Theta_m + \nabla\bullet\rho_m \vec{v}_m \Theta_m\right] = \bar{\bar{S}}_m : \nabla\vec{v}_m - \nabla\bullet\left(\kappa_m \nabla\Theta_m\right) - \gamma_m + \phi_{fm} \tag{13}$$

$$\kappa_m = f_5\left(\varepsilon_m, \rho_m, d_m, \Theta_m^{1/2}, e_m, \beta\right) \quad \gamma_m = f_6\left(\varepsilon_m, \rho_m, d_m, \Theta_m^{3/2}, e_m\right) \quad \phi_{fm} = f_7\left(\varepsilon_m, \rho_m, d_{p,m}, \Theta_m, \left|\vec{v}_f - \vec{v}_m\right|, \beta\right) \tag{14}$$

In the algebraic approach, instead solving the full equation (6) , the granular energy is obtained by equating the first term on the right hand side with the dissipation term.

The model where Eqs. (7), (8) and (13) are solved is the kinetic theory model, termed here as KTGF. Conversely, in the constant solids viscosity model (CVM) the solids pressure is defined as in Eq. (6) and the solids viscosity in either plastic and viscous regimes is set constant.

In the case of a mixture of particles, i.e., the polidisperse system, the packed bed void fraction ε^* is dependent of the maximum packing of the individual solids constituents, their diameters, and volumetric fractions, following the work of Yu and Standish (1987):

In the work of Syamlal and Obrien (1988) using the KFIX code only the solids pressure term was modeled and no granular energy was modeled. Conversely, in their work they used the Fedors and Landel (1979) model for estimating ε^*.

3. NUMERICAL METHODOLOGY

MFIX (Multiphase Flow with Interphase eXchanges) is an open source CFD code developed at the National Energy Technology Laboratory (NETL) for describing the hydrodynamics, heat transfer and chemical reactions in fluid-solids systems. It has been used for describing bubbling and circulating fluidized beds, spouted beds and gasifiers. MFIX calculations give transient data on the three-dimensional distribution of pressure, velocity, temperature, and species mass fractions.

The hydrodynamic model is solved using the finite volume approach with discretization on a staggered grid. A second order accurate discretization scheme was used and superbee scheme was adopted for discretization of the convective fluxes at cell faces for all equations in this work. With the governing equations discretized, a sequential iterative solver is used to calculate the field variables at each time step. The main numerical algorithm is an extension of SIMPLE. Modifications to this algorithm in MFIX include a partial elimination algorithm to reduce the strong coupling between the two phases due to the interphase transfer terms. Also, MFIX makes use of a solids volume fraction correction step instead of a solids pressure correction step which is thought to assist convergence in loosely packed regions. Finally, an adaptive time step is used to minimize computation time. See Syamlal (1998) for more details.

The grid employed after mesh refinement is depicted in Figure 2. The computer used in the numerical simulations was a PC with OpenSuse linux and Intel Quad Core processor.

In this work, the parameters for controlling the numerical solution (e.g., under-relaxation, sweep direction, linear equation solvers, number of iterations, residual tolerances) were kept as their default values. Also, for setting up the mathematical model, when not otherwise specified the code default values were used.

For generating the numerical results and comparison with experimental results, when not otherwise specified, all the default code values were used, referred here as baseline simulation. Moreover, for the baseline simulation we employed the Syamlal-O´Brien drag model (see Syamlal and O´Brien, 1993), the standard solid stress model, and slip and non-slip condition for solid and gas phase, correspondingly. The previous set of models will be referred in the results section as baseline simulation models.

The experimental conditions of Moritomi et al. (1982) were chosen for the computer simulations. These conditions are outlined in Table 1. The bed geometry was represented in two dimensions by axisymmetric cylindrical coordinates. Polidisperse simulations started from uniformly mixed beds.

Table 1. Computer simulation conditions.

Particles	d_p (mm)	ρ_s
Glass beads	0.163	2.45
Hollow char	0.775	1.5
Fluid (water)	$\rho_f = 1$ g/cm^3	$\mu_f = 0.01$ g/(cm s)
Bed dimensions		
Diameter	5.0 cm	
Height	30.0 cm	
Mesh	10×200	

4. RESULTS AND DISCUSSION

Figures 1(a) e 1(b) presents a comparison of the numerical and experimental results for the bulk density ($= \overline{\varepsilon_f}\rho_f + \overline{\varepsilon_m}\rho_f$) for the monodisperse beds. An analysis shows that the computed bulk densities of fluidized bed of glass beads agree reasonably well with experimental data and simulations by Syamlal and O´Brien for lower fluid velocities. The predicted values for the bulk density are greater than the experimental and Syamlal and O´Brien results. The last verification is also true for beds of hollow char.

Particle mixture simulations were carried out for overall bed composition of 100 g glass beads and 50 g hollow char. Figure (2) presents the time averaged solid volumetric profiles as a function of the height from the bed base. The layer of glass beads expands monotonically with increasing fluid velocity. At velocity of 0.35 cm/s, a comparison of the height of the profiles shows that exists a rich hollow char layer at the top of the bed. The profile for the glass bead reveals that a rich layer subsides to the bottom of the bed. At velocity of 0.93 cm/s the profile indicates that the glass beads are mostly segregated at the top of the bed. The later observation closely follows the scenario depicted in experiments by Moritomi et al. (1982), where at fluid velocity of 1 cm/s, the inversion velocity, the glass bead layer resides at the top of the bed.

Figure 3 shows the comparison with experimental data for the bed height with hollow char at the top. The results predicted by our simulations are lower than experimental. However, the rate of growth is roughly the same.

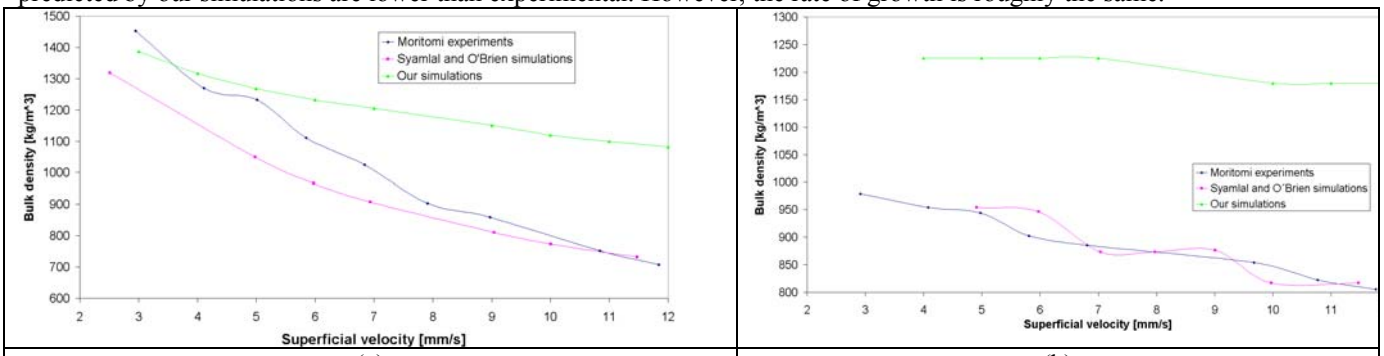

(a) (b)

Figure 1. Bulk densities comparison for monodisperse beds

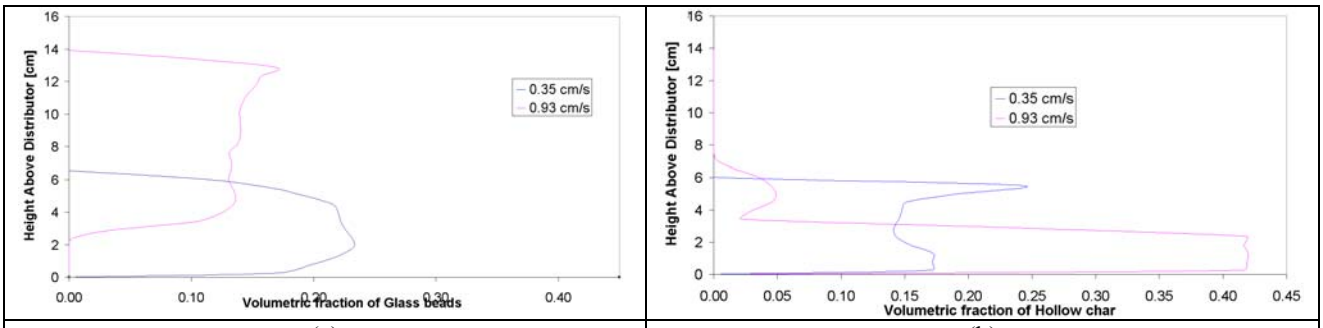

(a) (b)

Figure 2. Time averaged solid volumetric fraction distribution at two different fluid velocities for glass beads and hollow char

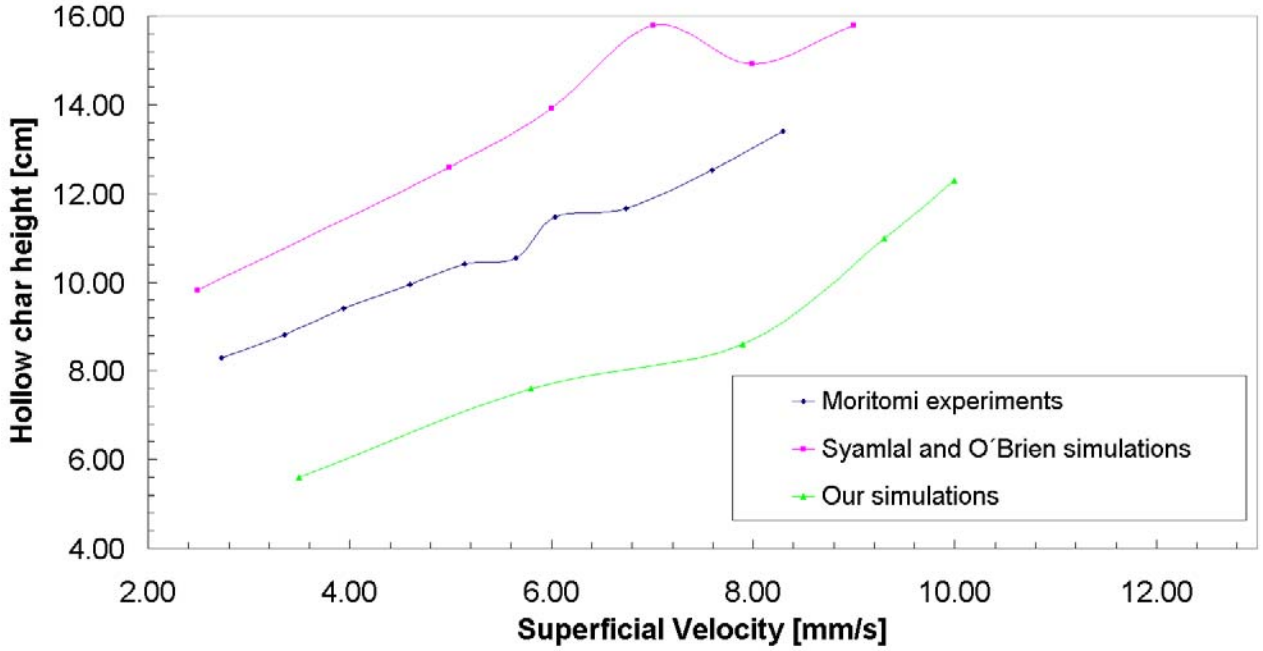

Figure 3. Bed height versus superficial velocity

5. CONCLUSION

We have presented a new attempt to study segregation in a liquid fluidized bed using a multiparticle numerical code with improvements in the underlying theory. Semiquantitative agreements with some limited experimental data and previous numerical simulation were obtained. Further verification/validation is on pursuit.

6. REFERENCES

Anderson, T. B., 1967, "A fluid mechanical description of fluidized beds: Equations of motion", Industrial Engineering Chemical Fundamentals, Vol 6, pp. 527-539.

Benyahia, S., 2008, "Validation study of two continuum granular frictional flow theories", Industrial Engineering Chemical Research, 47, 8926-8932.

Benyahia, S., Syamlal, M., O'Brien, T. J., "Summary of MFIX Equations 2005-4", 1 March 2006: <http://www.mfix.org/documentation/MfixEquations2005-4-1.pdf>.

Escudié, R., Epstein, N., Grace, J. R., Bi, H. T., 2006, "Layer inversion phenomenon in binary-solid liquid-fluidized beds: Prediction of the inversion velocity", Chemical Engineering Science, 61, 6667-6690.

Fedors, R. F., Landel, R. F., 1979, "Porosity calculations of multi-component mixtures of spherical particles", Powder Technology, 23, 225-231.

Moritomi, H., Iwase, T., Chiba, T., 1982, "A Comprehensive interpretation of solid layer inversion in liquid fluidised beds", Chemical Engineering Science, 37, 1751-1757.

Pannala, S., Daw, C. S., Finney, C. E. A., Benyahia, S., Syamlal, M., O´Brien, T. J., "Modelling the collisional-plastic stress transition for bin discharge of granular material", 2009, Powders and Grains 2009 – Proceeding of the 6th International Conference on Micromechanics of Granular Media, pp. 657-660.

Syamlal, M., 1998, "MFIX Documentation, Numerical Techniques", Technical Note, DOE/MC-31346-5824, NTIS/DE98002029, National Technical Information Service, Springfield, VA, USA.

Syamlal, M., O´Brien, T. J., 1988, "Simulation of granular layer inversion in liquid fluidized beds", International Journal of Multiphase Flow, 14, 473-481.

Syamlal, M., Pannala, S., Multiphase Continuum Formulation for Gas-Solids Reacting Flows. In : Pannala, S., Syamlal, M., O´Brien, T. J., Computational Gas-Solids Flow and Reacting Systems: Theory, Methods and Practice, Engineering Science Reference, IGI Global, cap 1, pp. 1-65, 2011.

Syamlal, M., Rogers, W. A., O'Brien, T. J., 1993, "MFIX Documentation, Theory Guide", Technical Note, DOE/METC-94/1004, NTIS/DE94000087, National Technical Information Service, Springfield, VA, USA.

Yu, A. B., Standish, N., 1987, "Porosity calculations of multi-component mixtures of spherical particles", Powder Technology, 52, 233-241.

7. RESPONSIBILITY NOTICE

The authors are the only responsible for the printed material included in this paper.